

## Platinum Complexes

## Boranediyl- and Diborane(4)-1,2-diyl-Bridged Platinum A-Frame Complexes

Carina Brunecker,<sup>[a]</sup> Jonas H. Müssig,<sup>[a]</sup> Merle Arrowsmith,<sup>[a]</sup> Felipe Fantuzzi,<sup>[a, b]</sup> Andreas Stoy,<sup>[a]</sup> Julian Böhnke,<sup>[a]</sup> Alexander Hofmann,<sup>[a]</sup> Rüdiger Bertermann,<sup>[a]</sup> Bernd Engels,<sup>[b]</sup> and Holger Braunschweig<sup>\*[a]</sup>

**Abstract:** Diplatinum A-frame complexes with a bridging (di)boron unit in the apex position were synthesized in a single step by the double oxidative addition of dihalo(di)borane precursors at a bis(diphosphine)-bridged Pt<sup>0</sup> complex. While structurally analogous to well-known  $\mu$ -borylene complexes, in which delocalized dative three-center-two-electron M-B-M bonding prevails, theoretical investigations into the nature of Pt–B bonding in these A-frame complexes show them to be rare dimetalla(di)boranes displaying two electron-sharing Pt–B  $\sigma$ -bonds. This is experimentally reflected in the low kinetic stability of these compounds, which are prone to loss of the (di)boron bridgehead unit.

In organometallic chemistry, transition metal carbene complexes are divided into two classes: a) Fischer carbenes, in which R<sub>2</sub>C–M bonding is governed by  $\sigma$  donation of the carbene lone pair into an empty metal orbital and  $\pi$  backdonation from a filled metal d orbital into the empty carbene p orbital, and b) Schrock carbenes, in which bonding occurs between a triplet R<sub>2</sub>C: carbene and a triplet-state metal center.<sup>[1]</sup> With their singlet ground state, which is independent of the nature of the substituent R,<sup>[2]</sup> and empty p orbitals, borylenes (RB<sub>2</sub>) may be considered as analogues of Fischer carbenes. Thus, the bonding in terminal borylene complexes is governed by  $\sigma$  donation from the borylene lone pair to the metal center

and  $\pi$  backbonding from the electron-rich metal center to the borylene, resulting in metal–boron multiple bonding.<sup>[3]</sup>

Like Schrock carbenes, however, borylenes are often found in bridging positions between two or more metal centers. Since the isolation of the first dinuclear bridging borylene complexes [ $\mu$ -(BY){ $\eta^5$ -(C<sub>5</sub>H<sub>5</sub>R)Mn(CO)<sub>2</sub>}]<sub>2</sub>] (Y=NMe<sub>2</sub>, R=H; Y=tBu, R=Me),<sup>[4]</sup> this class of compounds has been extensively studied in terms of electronic properties and reactivity.<sup>[3a–c]</sup> The nature of M–B–M bonding in borylene-bridged dimanganese complexes (**I**, Figure 1) was examined both experimentally and

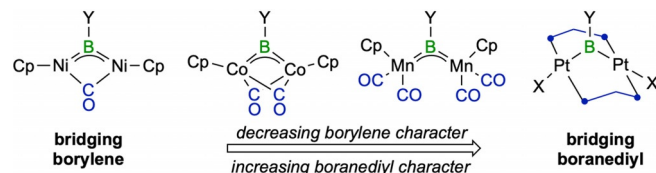


Figure 1. Bonding modes in homobimetallic  $\mu$ -BY-bridged complexes. Cp = cyclopentadienyl.

computationally. Instead of the delocalized three-center-two-electron (3c2e) dative bonding expected for bridging borylenes, the topological analysis of the electron density distribution from a low-temperature, high-resolution X-ray diffraction experiment suggested two localized, directional two-electron Mn–B bonds, leading the authors to describe these complexes as dimetallaboranes (or boranediyls).<sup>[5]</sup> Calculations based on the quantum theory of atoms in molecules (QTAIM) and on the electron-localization function (ELF) revealed that the calculated bonding situation—that is, borylene versus boranediyl—strongly depends on the choice of exchange-correlation functional.<sup>[5]</sup> Similar calculations on homodinuclear nickel (**II**) and cobalt (**III**)  $\mu$ -borylene complexes suggested that the dinickel complex should be described as a true bridging borylene whereas bonding in the dicobalt complex is closer to the boranediyl model, irrespective of the choice of density functional.<sup>[7]</sup> Additionally, complexes **I**–**III** are all stabilized by delocalization of the metal–metal bonding molecular orbital over the empty orbitals of the boron bridge and thus fulfil the 18 valence electron rule.

Since the nature of the M–B–M bonding in bridging “borylene” complexes remains complicated to determine both experimentally and computationally, we set out to synthesize true boranediyl complexes and compare their structure, elec-

[a] C. Brunecker, Dr. J. H. Müssig, Dr. M. Arrowsmith, Dr. F. Fantuzzi, A. Stoy, Dr. J. Böhnke, Dr. A. Hofmann, Dr. R. Bertermann, Prof. Dr. H. Braunschweig  
Institut für Anorganische Chemie and  
Institute for Sustainable Chemistry & Catalysis with Boron  
Julius-Maximilians-Universität Würzburg  
Am Hubland, 97074 Würzburg (Germany)  
E-mail: h.braunschweig@uni-wuerzburg.de

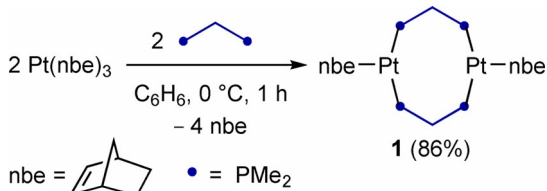
[b] Dr. F. Fantuzzi, Prof. Dr. B. Engels  
Institut für Physikalische und Theoretische Chemie  
Julius-Maximilians-Universität Würzburg  
Emil-Fischer-Straße 42, 97074 Würzburg (Germany)

Supporting information and the ORCID identification number(s) for the author(s) of this article can be found under:  
<https://doi.org/10.1002/chem.202001168>.

© 2020 The Authors. Published by Wiley-VCH Verlag GmbH & Co. KGaA.  
This is an open access article under the terms of the Creative Commons Attribution License, which permits use, distribution and reproduction in any medium, provided the original work is properly cited.

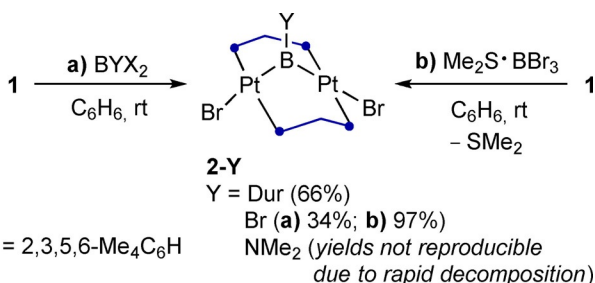
tronics and reactivity to known bridging borylenes. For this purpose, we chose so-called A-frame complexes,<sup>[8]</sup> in which the two metal centers are tethered by two bridging diphosphine ligands and a bridging apex ligand, and which generally show no metal-metal bonding interactions. In this communication we present the synthesis and characterization of a series of boranediyl platinum A-frame complexes (**IV**), as well as a unique diborane(4)-1,2-diyl complex, and undertake an in-depth computational analysis of the nature of bonding in the Pt-B-Pt bridge.

Our precursor for the desired boron-bridged platinum A-frames, complex **1**, was synthesized by reacting  $[\text{Pt}(\text{nbe})_3]$  ( $\text{nbe}$ =norbornene) with 2 equiv bis(dimethylphosphino)methane (dppm) at  $0^\circ\text{C}$  (Scheme 1). The  $^{31}\text{P}$  NMR spectrum of **1** shows a single resonance of higher order, similar to the literature-known complex  $[(\mu\text{-dppm})_3\text{Pt}_2]$  (dppm=bis(diphenylphosphino)methane).<sup>[9]</sup> In the solid state the  $\text{Pt}\cdots\text{Pt}$  distance of  $4.096(1)$  Å confirms the absence of  $\text{Pt}\cdots\text{Pt}$  bonding in **1**. To our knowledge, **1** is the only crystallographically characterized diphosphine-bridged dinuclear  $\text{Pt}^0$  complex without  $\text{Pt}\cdots\text{Pt}$  bonding.<sup>[10]</sup>

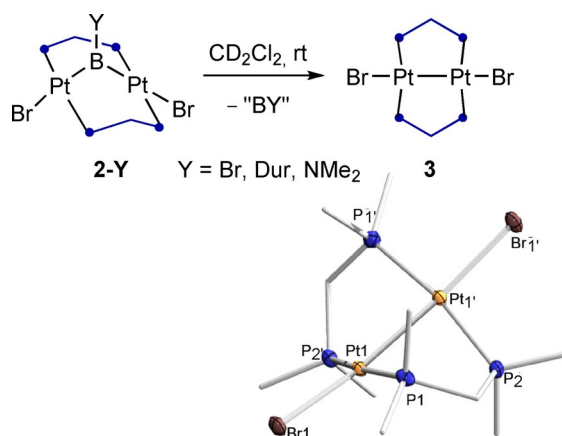


Scheme 1. Synthesis of diplatinum complex **1**.

Previous syntheses of terminal platinum borylene complexes have generally relied on the oxidative addition of  $\text{RBX}_2$  dihaloboranes to  $\text{Pt}^0$  centers to generate boryl complexes of the form  $[\text{L}_2\text{PtX}(\text{BXR})]$ , which were then converted to the corresponding cationic<sup>[11]</sup> or neutral borylenes<sup>[12]</sup> by halide abstraction or base-induced halide transfer to platinum, respectively. With this in mind, we carried out the room-temperature addition of dibromoboranes ( $\text{BYBr}_2$ ,  $\text{Y}=\text{Dur}=2,3,5,6\text{-Me}_4\text{C}_6\text{H}$ ,  $\text{Br}$ ,  $\text{NMe}_2$ ) to a benzene solution of complex **1**, which led to the instant formation of a yellow-orange precipitate (Scheme 2 a). Recrystallization from a dichloromethane/pentane mixture at room temperature yielded the  $\mu$ -borylene diplatinum A-frame complexes **2-Dur** (66%), **2-Br** (34%) and **2-NMe<sub>2</sub>**, the latter



Scheme 2. Synthesis of boranediyl-bridged diplatinum A-frame complexes.



Scheme 3. Decomposition of boranediyl complexes **2-Y** to **3** and crystallographically derived molecular structure of **3**. Thermal ellipsoids at 50% probability. Thermal ellipsoids of ligand periphery and hydrogen atoms omitted for clarity. Selected bond lengths (Å) and angles (°):  $\text{Pt1}\cdots\text{Pt1}'$  2.6163(4),  $\text{Pt1}\cdots\text{Br1}$  2.5189(5),  $\text{P1}\cdots\text{Pt1}\cdots\text{P2}'$  169.53(4),  $\text{Br1}\cdots\text{Pt1}\cdots\text{Pt1}'$  172.859(11), torsion angle  $\text{P1}\cdots\text{Pt1}\cdots\text{Pt1}'\cdots\text{P2}'$  49.41(4).

proving highly unstable in both solution and the solid state (Scheme 3). By employing the dimethylsulfide precursor  $\text{Me}_2\text{S}\cdot\text{BBr}_3$  instead of  $\text{BBr}_3$  the yield of **2-Br** became essentially quantitative (Scheme 2 b).

The  $^{11}\text{B}$  NMR spectra of **2-Y** show extremely broad resonances (full width at mid-height (fwmh)  $\approx 1200$  to  $2150$  Hz) at 98 (**2-Dur**), 85 (**2-Br**) and 52 ppm (**2-NMe<sub>2</sub>**), in line with the increasing electron-donating nature of the substituent at boron. These are significantly upfield-shifted compared to structurally related borylene-bridged bimetallic complexes ( $\mu\text{-BAr}$ :  $\delta_{11\text{B}}=122$  to  $162$  ppm;  $\mu\text{-BBr}$ :  $\delta_{11\text{B}}=107$  to  $163$  ppm;  $\mu\text{-BNR}_2$ :  $\delta_{11\text{B}}=70$  to  $119$  ppm).<sup>[3b, 13]</sup> It is noteworthy, however, that the  $^{11}\text{B}$  NMR resonances of platinum-containing heterobimetallic bridging borylenes,  $[\mu\text{-BY}\{\text{ML}_n\}(\text{PtL}_m)\}]$ , are generally 20 to 35 ppm upfield-shifted compared to the analogous homobimetallic complexes without platinum,  $[\mu\text{-BY}(\text{ML}_n)_2]$ ,<sup>[14]</sup> owing to the strongly electron-donating nature of the  $\text{Pt}^0$  center.

The  $^{31}\text{P}\{{}^1\text{H}\}$  NMR spectra of **2-Dur**, **2-Br** and **2-NMe<sub>2</sub>** showed singlets at  $-13.6$ ,  $-9.3$  and  $-5.6$  ppm, respectively, with a complex higher-order satellite motif. These arise from the superimposed spectra of isotopomers containing no  $^{195}\text{Pt}$  nuclei (43.8%, sharp singlet), one  $^{195}\text{Pt}$  nucleus (44.8%, AA'A''A'''X spin system), and two  $^{195}\text{Pt}$  nuclei (11.4%, AA'A''A'''XX' spin system), based on the natural abundance of these isotopes. Based on reported analyses of higher-order spectra in doubly dppm-bridged diplatinum complexes,<sup>[15]</sup> the  $^{31}\text{P}\{{}^1\text{H}\}$  NMR spectrum of **2-Br** (Figure 2) yields coupling constants of  $J_{\text{PPt}}=3270$  Hz,  $J_{\text{P1P2}}=220$  Hz,  $J_{\text{P1Pt}}=510$  Hz and  $Q=J_{\text{P1P2}}+J_{\text{P1P3}}=42$  Hz.<sup>[16]</sup> These coupling constants are similar to those observed for cationic  $\mu$ -hydride<sup>[15]</sup> and  $\mu$ -chloride-bridged<sup>[15b]</sup> and neutral  $\text{CH}_2$ -bridged<sup>[17]</sup>  $(\mu\text{-dppm})_2\text{Pt}_2$  A-frame complexes. The  $^{195}\text{Pt}\{{}^1\text{H}\}$  NMR spectrum of **2-Br** displays a higher-order multiplet at  $-3865$  ppm, additionally broadened by coupling to the quadrupolar boron nucleus, the analysis of which confirms the  $J_{\text{PPt}}$  coupling constant of around 3300 Hz.<sup>[18]</sup>

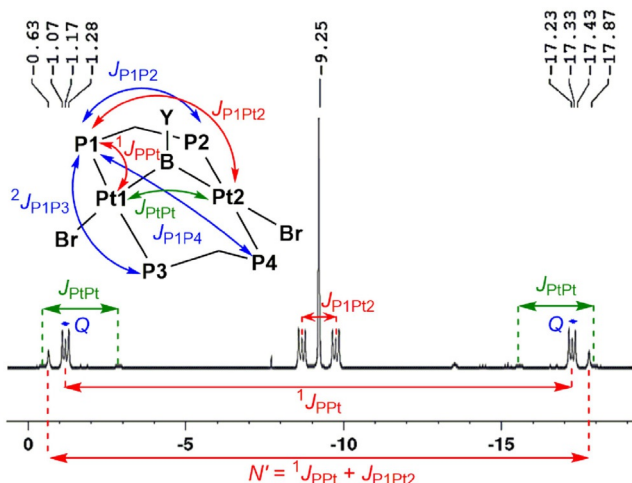


Figure 2. Annotated  $^{31}\text{P}\{\text{H}\}$  NMR spectrum of **2-Br**.

Figure 3 shows the solid-state structures of the 32-electron complexes **2-Dur**, **2-Br** and **2-NMe<sub>2</sub>**, in which the Pt–Pt distances (3.1347(9) to 3.4015(4) Å) clearly indicate the absence of Pt–Pt bonding. This contrasts with the only other known boryl-bridged  $(\mu\text{-dppm})_2\text{Pt}_2$  A-frame complexes,  $[\mu\text{-BCat}(\mu\text{-dppm})_2\text{Pt}_2(\text{BCat})(\text{PR}_3)]$  ( $\text{Cat}=\text{catecholate}$ ,  $\text{PR}_3=\text{PPh}_3$ ,  $\kappa_1\text{-dppm}$ ), isolated from the reaction of  $[(\text{PPh}_3)_2\text{Pt}(\text{BCat})_2]$  with excess dppm, in which the short Pt–Pt distance of 2.77 Å indicates Pt–Pt bonding.<sup>[19]</sup> Complex **2-Br** displays crystallographically imposed  $C_2$  symmetry with the symmetry axis passing through B1 and bisecting the Pt1...Pt1' vector, and virtually no distortion from an idealized A-frame, with the Pt centers in near square-planar environments and a P1-Pt1-Pt1'-P2 torsion angle

(−1.51(3)°) close to 0°. As the steric demands of the substituent at boron increase ( $\text{Br} < \text{NMe}_2 < \text{Dur}$ ) the geometry of the A-frame becomes increasingly distorted, with the P1-Pt1-Pt2-P4 torsion angles reaching around 26° in **2-Dur** (compare side-views of **2-Dur**, **2-Br** and **2-NMe<sub>2</sub>** in Figure 3). The Pt–Br bond length also increases in the order  $\text{Y} = \text{Br} < \text{BNMe}_2 < \text{Dur}$ , which is in line with the increase in *trans* effect previously determined for boryl ligands at square-planar Pt<sup>II</sup> complexes.<sup>[20]</sup> The boron atoms in the complexes **2-Y** are trigonal planar and the Pt–B bond lengths span the range from 1.967(3) (**2-Br**) to 2.042(9) Å (**2-NMe<sub>2</sub>**), which is within the range of known platinum-containing bimetallic bridging borylene complexes (1.910(4) to 2.091(4) Å).<sup>[14]</sup>

Given that the structural resemblance of **2-Y** with  $\mu$ -borylene complexes contrasts with the unusually upfield-shifted  $^{11}\text{B}$  NMR resonances, we analyzed the nature of the Pt–B bonding in **2-Dur**, **2-Br** and **2-NMe<sub>2</sub>** with the computational EDA-NOCV method.<sup>[21]</sup> The calculations were carried out considering two distinct scenarios: 1) the interaction of the  $\{(\mu\text{-dppm})\text{Pt}\}_2$  and BY fragments in their electronic triplet spin states, corresponding to the formation of electron-sharing Pt–B  $\sigma$  bonds in **2-Y**, and 2) the interaction of both fragments in their electronic singlet states, corresponding to borylene-type complexes with delocalized donor–acceptor bonding. For all **2-Y** compounds studied herein the second scenario yields a significantly larger orbital interaction than the first (see Tables S1–S3 in the Supporting Information for details), the smaller orbital interaction values indicating a more appropriate choice of fragments.<sup>[22]</sup> As a result, **2-Y** should be regarded as bridging boranediyl (or di-metallaborane) rather than delocalized three-center  $\mu$ -borylene complexes. In all cases, B–Pt bonding is dominated by electrostatic interactions (56 to 68%), with non-negligible contribu-

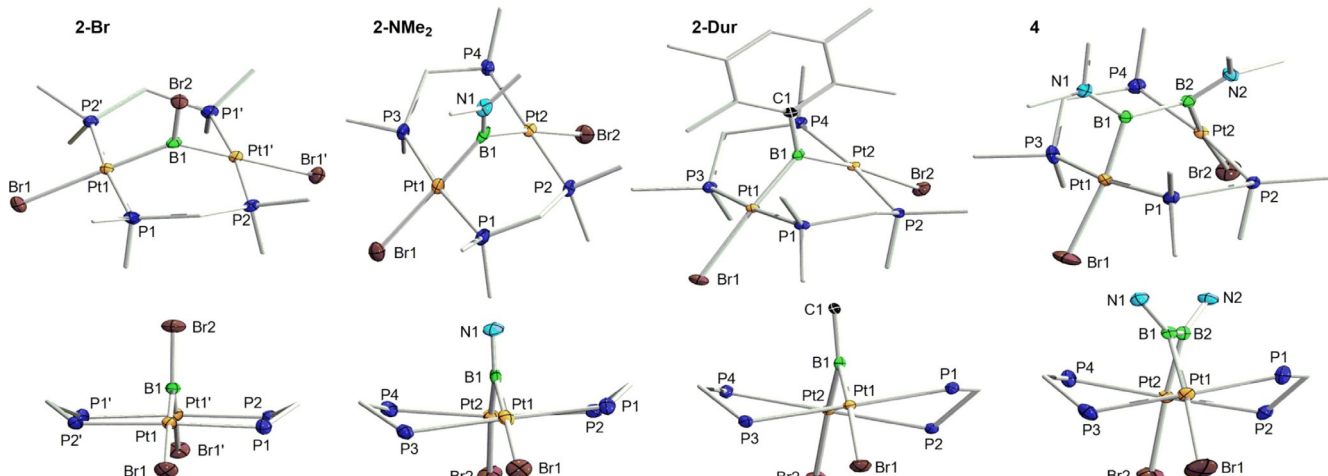


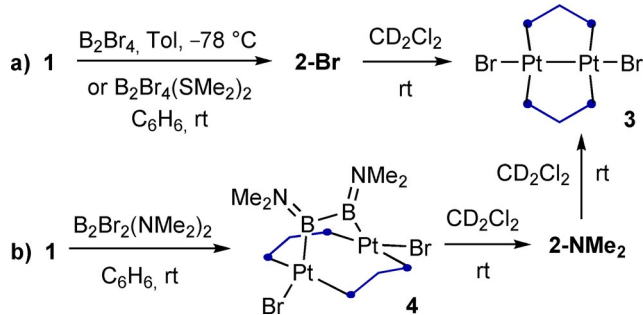
Figure 3. Top: Crystallographically derived molecular structures of (from left to right) **2-Br**, **2-NMe<sub>2</sub>**, **2-Dur** and **4**. Thermal ellipsoids at 50% probability. Thermal ellipsoids of ligand periphery and hydrogen atoms omitted for clarity. Bottom: Truncated side-views of the same complexes evidencing the increasing distortion of the A-frame through the increase of the P1/3-Pt1-Pt2-P2/4 torsion angle. Thermal ellipsoids of ligand periphery and all hydrogen atoms omitted for clarity. Selected bond lengths (Å) and angles (°) for **2-Br**: Pt1–Pt1' 3.4015(4), Pt1–B1 1.967(3), Pt1–Br1 2.6069(4), Pt1–B1–Pt1' 119.7(3), torsion angle Pt1–Pt1'–Pt2–P2 1.51(3) | **2-NMe<sub>2</sub>**: Pt1–Pt2 3.3003(4), Pt1–B1 2.028(10), Pt2–B1 2.042(9), B1–N1 1.395(12), Pt1–Br1 2.6298(9), Pt2–Br2 2.6236(9), Pt–B1–Pt2 108.4(5), torsion angles P1–Pt1–Pt2–P2 4.96(7), P3–Pt1–Pt2–P4 15.62(8) | **2-Dur**: Pt1–Pt2 3.1347(9), Pt1–B1 2.020(4), Pt2–B1 2.029(4), Pt1–Br1 2.6431(9), Pt2–Br2 2.6282(6), Pt–B1–Pt2 101.46(18), torsion angles P1–Pt–Pt2–P2 26.59(3), P3–Pt1–Pt2–P4 25.37(3) | **4**: Pt1–Pt2 3.372(1), Pt1–B1 2.085(6), Pt2–B2 2.100(6), B1–B2 1.687(8), B1–N1 1.418(7), B2–N2 1.467(7), Pt1–Br1 2.6609(11), Pt2–Br2 2.6901(13), Pt1–B1–B2 112.5(4), Pt2–B2–B1 109.8(4),  $\Sigma_{B_1} 359.1(4)$ ,  $\Sigma_{B_2} 359.7(4)$ , torsion angles P1–Pt–Pt2–P2 27.29(6), P3–Pt–Pt2–P4 27.60(6).

tions coming from orbital interactions. These result mainly from  $\Delta E_{\text{orb}(1)}$  and  $\Delta E_{\text{orb}(2)}$ , that is, the electron-sharing B–Pt  $\sigma$ -bonds (Figure 4b,c), while  $\Delta E_{\text{orb}(3)}$  is related to  $\pi$  backdonation from the Pt atoms to boron (Figure 4d), and accounts for merely 6 to 9% of the orbital interaction stabilization. Therefore, in contrast to complexes **II** and **III** (Figure 1), there is no significant stabilization of the boron bridgehead through delocalized  $\pi$  backbonding in **2-Y**.

Whereas many  $\mu$ -borylene complexes, especially aminoborylenes, tend to be very stable,<sup>[4,23]</sup> the boranediyls **2-Y** slowly decomposed in solution, the only identifiable decomposition product being the 30-electron  $[(\mu\text{-dppm})_2\text{Pt}_2\text{Br}_2]$  complex **3** (Scheme 3). The stability of **2-Y** decreased in the order of  $\text{Y} = \text{Br} > \text{Dur} \gg \text{NMe}_2$ , that is, with the increasing electron-donating nature of Y. While this decomposition occurs with formal loss of „BY“, no  $^{11}\text{B}$  NMR resonance of any decomposition by-product was detected.<sup>[24]</sup> This is reminiscent of the decomposition of boryl complexes *trans*- $[(\text{Cy}_3\text{P})_2\text{Pd}(\text{Br})(\text{BR}_2)]$  into *trans*- $[(\text{Cy}_3\text{P})_2\text{PdBr}_2]$  and *trans*- $[(\text{Cy}_3\text{P})_2\text{Pd}(\text{Br})\text{H}]$ , in which the fate of the boryl ligand and the origin of the palladium-bound hydride remains unclear.<sup>[25]</sup> In contrast, platinum boryl complexes tend to be very stable as the Pt–B bond is remarkably resistant even to hydrolysis.<sup>[26]</sup>

When treated with 1,2-dihaloboranes(4),  $\text{Pt}^0$  complexes are known to form diborane(4)yl complexes by (sometimes reversible) oxidative addition of the boron–halogen bond<sup>[27]</sup> or bis(boryl) complexes by oxidative addition of the B–B bond.<sup>[27b,28]</sup> When attempting to synthesize diboron-bridged complexes in

a similar manner from the reaction of **1** with 1,2-dihaloboranes(4), no reaction was observed with 1,2-dibromo-1,2-diduryldiborane(4), while the reaction with  $\text{B}_2\text{Br}_4$  resulted solely in the formation of **2-Br** (Scheme 4a). This is reminiscent of the syntheses of the first bridging borylene complexes from  $\text{B}_2\text{Cl}_2\text{Y}_2$  ( $\text{Y} = \text{NMe}_2$ ,  $\text{tBu}$ ) and two equivalents of  $\text{K}[(\text{C}_5\text{H}_4\text{R})\text{MnR}'(\text{CO})_2]$  ( $\text{R} = \text{H}, \text{Me}; \text{R}' = \text{H}, \text{SiMe}_2\text{Ph}$ ), in which the second BY moiety was lost as the corresponding diborane(6) derivative  $(\text{YBH}_2)_2$ .<sup>[4,29]</sup> The reaction of **1** with  $\text{B}_2\text{Br}_2(\text{NMe}_2)_2$ , however, yielded a mixture of **2-NMe<sub>2</sub>** ( $\delta_{11\text{B}} = 52$  ppm,  $\delta_{31\text{P}} = -5.6$  ppm) and a new species, complex **4**, displaying a  $^{31}\text{P}$  NMR singlet at  $-13.1$  ppm ( $^1J_{\text{PPt}} = 3383$  Hz) and a single, very broad  $^{11}\text{B}$  NMR resonance at  $58$  ppm ( $\text{fwhm} \approx 2000$  Hz). This is similar to the  $^{11}\text{B}$  NMR shift of  $55.6$  ppm displayed by  $[\mu\text{-}\{\text{B}_2(\text{NMe}_2)_2\}\{\text{PEt}_3\}_2\text{PtI}]_2$ , which is obtained from the 1:2 molar addition of  $\text{B}_2\text{I}_2(\text{NMe}_2)_2$  to  $[\text{Pt}(\text{PEt}_3)_2]$ ,<sup>[27a]</sup> and suggests that **4** is also a  $\mu$ -bridging diborane(4)-1,2-diyl complex (Scheme 4b).



Scheme 4. Reactions of **1** with diboranes(4). Tol = toluene.

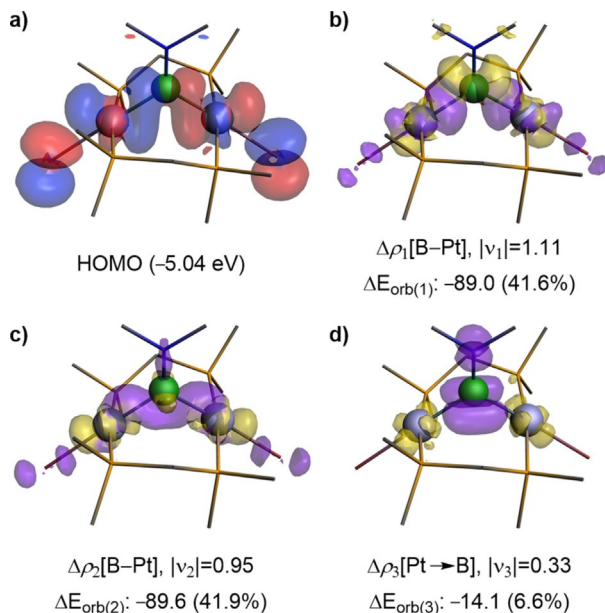


**Figure 4.** a) Plot of the HOMO of **2-NMe<sub>2</sub>** at the B3LYP/TZV2P// $\omega$ B97XD/cc-pVDZ,aug-cc-pVDZ-PP/Pt level of theory. b-d) Plot of deformation densities ( $\Delta\rho_i$ ) at the same level of theory, of the main orbital interactions of **2-NMe<sub>2</sub>**, starting from fragments  $[(\mu\text{-dppm})\text{Pt}_2]$  and BY in their electronic triplet state. The  $|\nu_i|$  values correspond to the eigenvalues of the complementary eigenfunctions ( $\psi_i, \psi_j$ ) in the NOCV representation, while  $\Delta E_{\text{orb}(i)}$  is the energy contribution ( $\text{kcal mol}^{-1}$ ) of the respective orbital interaction to the total orbital interaction energy,  $\Delta E_{\text{orb}}$ . The electron density flows from yellow to purple. Hydrogen atoms are omitted for clarity.

This was confirmed by the X-ray crystallographic analysis of colorless single crystals of **4** (Figure 3), the structure of which exhibits two platinum centers bridged by the *cis*-1,2-diaminodiborane(4)-1,2-diyl unit. The  $\text{Pt}_1\cdots\text{Pt}_2$  distance of **4** ( $3.372(1)$  Å) is only  $0.07$  Å longer than that of **2-NMe<sub>2</sub>** ( $3.3003(4)$  Å) and is actually shorter than that of **2-Br** ( $3.4015(4)$  Å) despite the additional aminoboryl unit in the bridge. The complex displays a strong distortion of its A-frame geometry, with P1-Pt1-Pt2-P2 and P3-Pt1-Pt2-P4 torsion angles of around  $27^\circ$  (see side-view of **4** in Figure 3). It is noteworthy that, whereas the B–B bond in  $[\mu\text{-}\{\text{B}_2(\text{NMe}_2)_2\}\{\text{PEt}_3\}_2\text{PtI}]_2$  ( $1.783(7)$  Å)<sup>[27a]</sup> is significantly longer than that of the  $\text{B}_2\text{I}_2(\text{NMe}_2)_2$  precursor ( $1.684(6)$  Å),<sup>[27d]</sup> the B–B bond in **4** ( $1.687(8)$  Å) is of a similar length to that in  $\text{B}_2\text{Br}_2(\text{NMe}_2)_2$  ( $1.682(16)$  Å),<sup>[30]</sup> the elongation likely being prevented by the geometry imposed by the A-frame. Like complexes **2-Y** complex **4** proved very unstable in solution and in the solid state, decomposing to **2-NMe<sub>2</sub>** and ultimately to **3**.<sup>[31]</sup> Since  $[\mu\text{-}\{\text{B}_2(\text{NMe}_2)_2\}\{\text{PEt}_3\}_2\text{PtI}]_2$  did not display any sign of decomposition in solution up to  $100^\circ\text{C}$ ,<sup>[27a]</sup> we surmise that the instability of **4**, and presumably also of **2-Y**, is caused by the strain of the A-frame geometry rather than an intrinsic instability of diplatinum (di)boranediyls.

The  $\mu$ -(diborane-1,2-diyl) character of **4** is also supported by EDA-NOCA calculations (see Table S4 and Figure S25 in the Supporting Information). Similar to **2-Y**, the  $\Delta E_{\text{orb}}$  term indi-

cates a preference of electron-sharing over donor-acceptor Pt–B bonds. The bonding is again dominated by electrostatic interactions (66.5%, see Supporting Information), with negligible  $\pi$  backdonation ( $\Delta E_{\text{orb}(4)} = 3.4\%$  of the orbital interaction stabilization) from Pt to B.

It is noteworthy that the formation of **2**–**Y** and **4** involves the highly selective, simultaneous oxidative *trans*-addition of a B–Br bond at each of the two  $\text{Pt}^0$  centers. Computational analyses by Zeng and Sakaki on the mechanism of oxidative *trans*-addition of  $\text{BBr}_2(\text{OSiMe}_3)$  to  $\text{Pt}(\text{PMe}_3)_2$  have shown that, following pre-coordination of the electron-deficient borane to the electron-rich  $\text{Pt}^0$  center, the addition of the B–Br bond may occur through one of two pathways: a) dissociation of  $\text{Br}^-$  to form a tightly bound  $[\text{Pt}(\text{PMe}_3)_2\{\text{BBr}(\text{OSiMe}_3)\}]^+[\text{Br}]^-$  ion pair, followed by direct nucleophilic attack of  $\text{Br}^-$  at the *trans* position, or b) oxidative *cis* addition, followed by thermal, rate-limiting *cis-trans* isomerization, the latter being slightly less favorable.<sup>[32]</sup> While it is likely that a similar mechanism takes place here, further computational studies beyond the scope of this communication would be required to determine whether this occurs in a fully concerted or stepwise manner, following either pathway a) or b).

To conclude, we have isolated a series of diplatinum borane-diyli and diborane-1,2-diyli A-frame complexes, all of which proved highly unstable and prone to loss of the boron bridge. DFT calculations showed that the metal–boron bonds in these complexes are electron-sharing  $\sigma$  bonds, with negligible contribution coming from  $\pi$  backdonation. This is in stark contrast with structurally related bridging borylenes, which display delocalized metal-to-boron  $\pi$  backbonding. Having thus established that the double oxidative addition of boron–halogen bonds at two tethered low-valent metal centers provides a reliable synthetic platform for accessing these rare dimetallated (di)boranes, we expect that variations in the nature of the metal centers and/or bridging ligand framework should yield in future, more stable, (di)boranediyls, the reactivity of which remains to be discovered.

## Experimental Section

**Crystallographic data:** Deposition numbers 1986723, 1986724, 1986725, 1986726, 1986727, and 1986728 contain the supplementary crystallographic data for this paper. These data are provided free of charge by the joint Cambridge Crystallographic Data Centre and Fachinformationszentrum Karlsruhe Access Structures service.

## Acknowledgements

This project was funded by the Deutsche Forschungsgesellschaft. F.F. thanks the Coordenação de Aperfeiçoamento de Pessoal de Nível Superior (CAPES) and the Alexander von Humboldt (AvH) Foundation for a CAPES-Humboldt postdoctoral fellowship.

## Conflict of interest

The authors declare no conflict of interest.

**Keywords:** boron · bonding · EDA-NOCV · oxidative addition · platinum

- [1] a) P. de Frémont, N. Marion, S. P. Nolan, *Coord. Chem. Rev.* **2009**, *293*, 862–892; b) G. Frenking, M. Solàb, S. F. Vyboishchikov, *J. Organomet. Chem.* **2005**, *690*, 6178–6204.
- [2] a) M. Krasowska, H. F. Bettinger, *J. Am. Chem. Soc.* **2012**, *134*, 17094–17103; b) M. Krasowska, M. Edelmann, H. F. Bettinger, *J. Phys. Chem. A* **2016**, *120*, 6332–6341.
- [3] a) J. T. Goettel, H. Braunschweig, *Coord. Chem. Rev.* **2019**, *380*, 184–200; b) H. Braunschweig, R. D. Dewhurst, V. H. Gessner, *Chem. Soc. Rev.* **2013**, *42*, 3197–3208; c) H. Braunschweig, R. D. Dewhurst, A. Schneider, *Chem. Rev.* **2010**, *110*, 3924–3957; d) H. Braunschweig, C. Kollann, F. Seeler, *Struct. Bond.*, eds. T. B. Marder, Z. Lin, **2008**, *130*, 1–28, Springer-Verlag Berlin Heidelberg; e) H. Braunschweig, C. Kollann, U. Englert, *Angew. Chem. Int. Ed.* **1998**, *37*, 3179–3180; *Angew. Chem.* **1998**, *110*, 3355–3357.
- [4] a) H. Braunschweig, B. Ganter, *J. Organomet. Chem.* **1997**, *545*, 163–167; b) H. Braunschweig, T. Wagner, *Angew. Chem. Int. Ed. Engl.* **1995**, *34*, 825–826; *Angew. Chem.* **1995**, *107*, 904–905.
- [5] U. Fließer, M. Burzler, D. Leusser, J. Henn, H. Ott, H. Braunschweig, D. Stalke, *Angew. Chem. Int. Ed.* **2008**, *47*, 4321–4325; *Angew. Chem.* **2008**, *120*, 4393–4397.
- [6] K. Götz, M. Kaupp, H. Braunschweig, D. Stalke, *Chem. Eur. J.* **2009**, *15*, 623–632.
- [7] H. Braunschweig, B. Christ, M. Colling-Hendelkens, M. Forster, K. Götz, M. Kaupp, K. Radacki, F. Seeler, *Chem. Eur. J.* **2009**, *15*, 7150–7155.
- [8] a) D. M. Hoffmann, R. Hoffmann, *Inorg. Chem.* **1981**, *20*, 3543–3555; b) C. P. Kubiak, R. Eisenberg, *J. Am. Chem. Soc.* **1977**, *99*, 6129–6131.
- [9] L. Manojlović-Muir, K. W. Muir, M. C. Grossel, M. P. Brown, C. D. Nelson, A. Yavari, E. Kallas, R. P. Moulding, K. R. Seddon, *J. Chem. Soc. Dalton Trans.* **1986**, 1955–1963.
- [10] In solution at 60 °C, **1** decomposed rapidly, which is likely due to the absence of stabilizing Pt–Pt interaction.
- [11] a) N. Arnold, H. Braunschweig, P. B. Brenner, R. Dewhurst, T. Kramer, K. Radacki, *Organometallics* **2015**, *34*, 2343–2347; b) N. Arnold, H. Braunschweig, P. Brenner, J. O. C. Jimenez-Halla, T. Kupfer, K. Radacki, *Organometallics* **2012**, *31*, 1897–1907; c) H. Braunschweig, K. Radacki, K. Uttinger, *Organometallics* **2008**, *27*, 6005–6012; d) H. Braunschweig, K. Radacki, K. Uttinger, *Angew. Chem. Int. Ed.* **2007**, *46*, 3979–3982; *Angew. Chem.* **2007**, *119*, 4054–4057; e) H. Braunschweig, K. Radacki, D. Rais, D. Scheschkowitz, *Angew. Chem. Int. Ed.* **2005**, *44*, 5651–5654; *Angew. Chem.* **2005**, *117*, 5796–5799.
- [12] a) H. Braunschweig, P. Brenner, R. D. Dewhurst, K. Radacki, *Z. Naturforsch. B* **2013**, *68*, 747–749; b) H. Braunschweig, P. Brenner, K. Radacki, *Z. Anorg. Allg. Chem.* **2009**, *635*, 2089–2092.
- [13] H. Braunschweig, M. Colling, *Eur. J. Inorg. Chem.* **2003**, 393–403.
- [14] a) H. Braunschweig, T. Kramer, *Acta Crystallogr. Sect. E* **2014**, *70*, 421–423; b) H. Braunschweig, A. Damme, K. Radacki, Q. Ye, *Chem. Commun.* **2013**, *49*, 7593–7595; c) H. Braunschweig, M. Burzler, T. Kupfer, K. Radacki, F. Seeler, *Angew. Chem. Int. Ed.* **2007**, *46*, 7785–7787; *Angew. Chem.* **2007**, *119*, 7932–7934; d) H. Braunschweig, K. Radacki, K. Uttinger, *Eur. J. Inorg. Chem.* **2007**, 4350–4356; e) H. Braunschweig, K. Radacki, D. Rais, K. Uttinger, *Organometallics* **2006**, *25*, 5159–5164; f) H. Braunschweig, K. Radacki, D. Rais, F. Seeler, *Angew. Chem. Int. Ed.* **2006**, *45*, 1066–1069; *Angew. Chem.* **2006**, *118*, 1087–1090.
- [15] a) M. C. Grossel, J. R. Batson, R. P. Moulding, K. R. Seddon, *J. Organomet. Chem.* **1986**, *304*, 391–423; b) M. P. Brown, R. J. Puddephatt, L. Rashidi, K. R. Seddon, *J. Chem. Soc. Dalton Trans.* **1978**, 516–522.
- [16] Where  $J_{\text{P1P2}} = {}^3J(\text{PCH}_2\text{PPt}) + {}^3J(\text{PPtBPt})$ ,  $J_{\text{P1P2}} = {}^2J(\text{PCH}_2\text{P}) + {}^4J(\text{PPtBPtP})$  and  $J_{\text{P1P3}} = {}^2J(\text{PCH}_2\text{PPtP}) + {}^4J(\text{PPtBPtP})$ .
- [17] M. P. Brown, J. R. Fisher, S. J. Franklin, R. J. Puddephatt, K. R. Seddon, *J. Organomet. Chem.* **1978**, *161*, C46–C48.

- [18] A  $^{195}\text{Pt}\{\text{H}, \text{B}\}$  spectrum acquired on a 300 MHz NMR spectrometer fitted with a TBO probe did not yield significant improvement in the resolution as the signal-to-noise ratio was too small.
- [19] D. Curtis, M. J. G. Lesley, N. C. Norman, A. G. Orpen, J. Starbuck, *J. Chem. Soc. Dalton Trans.* **1999**, 1687–1694.
- [20] a) H. Braunschweig, P. Brenner, A. Müller, K. Radacki, D. Rais, K. Uttinger, *Chem. Eur. J.* **2007**, 13, 7171–7176; b) J. Zhu, Z. Lin, T. B. Marder, *Inorg. Chem.* **2005**, 44, 9384–9390.
- [21] M. P. Mitoraj, A. Michalak, T. Ziegler, *J. Chem. Theory Comput.* **2009**, 5, 962–975.
- [22] a) S. Sinhababu, S. Kundu, M. M. Siddiqui, A. N. Paesch, R. Herbst-Irmer, B. Schwederski, P. Saha, L. Zhao, G. Frenking, W. Kaim, D. Stalke, H. W. Roesky, *Chem. Commun.* **2019**, 55, 4534–4537; b) L. Zhao, M. Hermann, N. Holzmann, G. Frenking, *Coord. Chem. Rev.* **2017**, 344, 163–204.
- [23] a) K. Geetharani, S. K. Bose, B. Varghese, S. Ghosh, *Chem. Eur. J.* **2010**, 16, 11357–11366; b) H. Braunschweig, M. Koster, *J. Organomet. Chem.* **1999**, 588, 231–234; c) A. W. Ehlers, E. J. Baerends, F. M. Bickelhaupt, U. Radius, *Chem. Eur. J.* **1998**, 4, 210–221.
- [24] In all cases the formation of **3** was accompanied by that of an insoluble precipitate, which may result from the polymerization of “BY”.
- [25] H. Braunschweig, K. Gruß, K. Radacki, K. Uttinger, *Eur. J. Inorg. Chem.* **2008**, 1462–1466.
- [26] H. Braunschweig, K. Radacki, D. Rais, A. Schneider, F. Seeler, *J. Am. Chem. Soc.* **2007**, 129, 10350–10351.
- [27] a) H. Braunschweig, R. Bertermann, A. Damme, T. Kupfer, *Chem. Commun.* **2013**, 49, 2439–2441; b) H. Braunschweig, A. Damme, T. Kupfer, *Chem. Eur. J.* **2013**, 19, 14682–14686; c) H. Braunschweig, A. Damme, T. Kupfer, *Inorg. Chem.* **2013**, 52, 7822–7824; d) H. Braunschweig, A. Damme, T. Kupfer, *Chem. Eur. J.* **2012**, 18, 15927–15931; e) H. Braunschweig, A. Damme, T. Kupfer, *Angew. Chem. Int. Ed.* **2011**, 50, 7179–7182; *Angew. Chem.* **2011**, 123, 7317–7320.
- [28] J. H. Müssig, D. Prieschl, A. Deißenberger, R. D. Dewhurst, M. Dietz, J. O. C. Jiménez-Halla, A. Trumpp, S. R. Wang, C. Brunecker, A. Häfner, A. Gärtnner, T. Thiess, J. Böhnke, K. Radacki, R. Bertermann, T. B. Marder, H. Braunschweig, *J. Am. Chem. Soc.* **2018**, 140, 13056–13063.
- [29] H. Braunschweig, M. Burzler, R. Dewhurst, K. Radacki, F. Seeler, *Z. Anorg. Allg. Chem.* **2008**, 634, 1875–1879.
- [30] A. Moezzi, M. M. Olmstead, P. P. Power, *J. Chem. Soc. Dalton Trans.* **1992**, 2429–2434.
- [31] See Figure S21 in the Supporting Information for a stack-plot of  $^{31}\text{P}$  NMR spectra of the decomposition of **4** in  $\text{CD}_2\text{Cl}_2$  over a period of 3 days at rt.
- [32] G. Zeng, S. Sakaki, *Inorg. Chem.* **2011**, 50, 5290–5297.

Manuscript received: March 6, 2020

Revised manuscript received: March 20, 2020

Accepted manuscript online: March 20, 2020

Version of record online: June 17, 2020